

## **Rill erosion on a sandy soil: preliminary field experiment and quasi-3D numerical simulation**

**STEFANO FERRARIS, GIUSEPPE CARRA**

*Dip. Economia e Ingegneria Agraria, Forestale e Ambientale, Universita di Torino, I-10095 Grugliasco, Italy*

**CLAUDIO GALLO**

*CRS4 Centro di Ricerca per la Sardegna, Cagliari, Italy*

**GIANMARCO MANZINI**

*Istituto d'Analisi Numerica, CNR, Pavia, Italy*

**Abstract** This paper illustrates the validation of a quasi three-dimensional model of overland flow and soil erosion phenomena by comparing numerical investigations with the results of an *ad hoc* designed field experiment. The model couples a shock capturing finite-volume approximate solution of a kinematic wave and soil transport rill model with a two-dimensional finite element solution of a variably saturated Richards' equation on the vertical plane perpendicular to the rill. The rill is 2 m long on a sandy hill with a 9% slope. Preliminary results show a good agreement between measured and simulated discharges.

### **INTRODUCTION**

Rill erosion is one of the most important processes responsible for soil loss and sediment production. Its hydraulics behaviour has been studied in detail in recent works. Many experimental investigations have tried to point out the main parameters in the rill erosion process (e.g. Nearing *et al.*, 1997), but only in a few papers are experimental data compared with physically-based models of the whole surface-subsurface system (Hairsine & Rose, 1992; Sharda & Singh, 1994).

In this preliminary work, we illustrate the results of an experiment investigation suitably designed for the validation of a numerical model, which couples a surface channel model, a subsurface variably saturated soil model and a surface sediment transport model.

### **THE MODEL**

In the present section the complete system of equations is presented. All the equations are formulated according to the same system of coordinates, which assumes that the horizontal coordinate  $x$  is oriented normal to the rill direction, the coordinate  $y$  is downward oriented along the rill direction and the coordinate  $z$  is downward oriented in the direction normal to both  $x$  and  $y$  (Fig. 1).

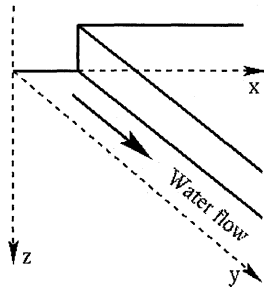


Fig. 1 Geometrical description of the rill.

The overland flow (Sharda & Singh, 1994) is described by the nonlinear hyperbolic equation:

$$\frac{\partial h}{\partial t} + \alpha m h^{m-1} \frac{\partial h}{\partial y} = i(t) - q(t) \quad (1)$$

where  $h$  is the water storage per unit area [L],  $i$  the rainfall intensity [ $L T^{-1}$ ],  $q$  the infiltration flux [ $L T^{-1}$ ],  $\alpha$  [ $L^{2-m} T^{-1}$ ] and  $m$  [-] are overland flow parameters ( $m = 5/3$  in the case of turbulent flow).

The subsurface flow in the variably saturated zone is described as reported in Paniconi & Putti (1994) by:

$$C(\psi) \frac{\partial \psi}{\partial t} = \frac{\partial}{\partial x} \left[ K(\psi) \left( \frac{\partial(\psi - z)}{\partial x} \right) \right] + \frac{\partial}{\partial z} \left[ K(\psi) \left( \frac{\partial(\psi - z)}{\partial z} \right) \right] \quad (2)$$

which is also known as Richards' equation. In this equation,  $\psi$  is the matric potential (L),  $\theta$  is the volumetric water content ( $L^3 L^{-3}$ ),  $K(\psi)$  is the hydraulic conductivity ( $L T^{-1}$ ),  $C(\psi) = \partial\theta/\partial\psi$  is the capillary capacity ( $L^3 L^{-4}$ ). We considered as the retention and conductivity curves the ones respectively proposed by van Genuchten (1980) and by Brooks & Corey (1964).

The overland erosion is described by a mass balance equation which states the conservation of the eroded soil transported by the rill flow:

$$\frac{\partial(AC_s)}{\partial t} + \frac{\partial(QC_s)}{\partial y} = e(y, t) \quad (3)$$

in which  $C_s$  is the volumetric sediment concentration ( $L^3 L^{-3}$ ),  $A$  is the flow cross-sectional area,  $Q$  is the liquid discharge ( $L^3 T^{-1}$ ) and  $e(y, t)$  is the rate of erosion of the soil bed ( $L^3 L^{-1} T^{-1}$ ). This latter term is generally composed of two parts, the first one, which accounts for the rain splash contribution and the other one for the hydraulic drag onto the bottom of the rill. In our experiment we do not have the rain contribution, whilst the hydraulic one is given by:

$$e(y, t) = c_g (C_{\max} - C_s) A \quad (4)$$

where  $c_g$  is a transfer rate coefficient computed by data regression, and  $C_{\max}$  is the concentration-at-equilibrium transport capacity, given by some empirical relations.

## THE NUMERICAL SOLUTION

The overland flow equation is solved by using a second-order Godunov-type shock capturing scheme. Let us introduce a partition of the domain of computation  $(a,b)$  for the coordinate  $y$  in  $N$  subintervals  $[y_i - \Delta y/2, y_i + \Delta y/2]$  of equal length  $\Delta y$ , where the nodes of the partition  $y_i$  are also equally spaced by  $\Delta y$ . Equation (1) is then reformulated in an integral conservative form on each subinterval:

$$\int_{y_i - \Delta y/2}^{y_i + \Delta y/2} \frac{\partial h}{\partial t} dy + \int_{y_i - \Delta y/2}^{y_i + \Delta y/2} \frac{\partial f(h)}{\partial y} dy = \int_{y_i - \Delta y/2}^{y_i + \Delta y/2} q dy \quad (5)$$

where  $f(h) = \alpha h^m$  is the physical flux function. The discretized form of equation (5) is:

$$\frac{\partial \bar{h}_i}{\partial t} + \frac{1}{\Delta y} (\hat{f}_{i+1/2} - \hat{f}_{i-1/2}) = \frac{1}{\Delta y} \bar{q}_i, \quad i = 0, N-1 \quad (6)$$

where  $\bar{h}_i$  and  $\bar{q}_i$  are the  $i$ th cell-averaged values of the conserved quantity  $h$  and the source term  $q$  and  $\hat{f}_{i+1/2}$  is the numerical flux function evaluated at the cell interface between cells  $i$  and  $i + 1$ . A MUSCL piecewise-linear reconstruction of the approximate solution, monotized by Colella's limiter, is used to estimate  $\hat{f}_{i+1/2}$  (Colella, 1990). The space-discretized equation is advanced in time by applying a second-order-in-time explicit Runge-Kutta scheme, conditionally stable according to a Courant-Friedrichs-Lewy constraint.

The Richards' equation is numerically solved by a finite element approach, which is summarized in the current section. For a detailed presentation of the method, when applied to groundwater flow and transport problems, we refer the reader to Pinder & Gray (1977).

The approximate solution  $\hat{\psi}(x, z, t)$  of the Richards' equation at any time  $t$  in the spatial domain  $\Omega \in R \times R$  is given in equation (7) as a linear combination of the basis functions  $N_l = N_l(x, z)$ . These latter ones forms the set of basis functions for the linear interpolation with Lagrangian polynomials on the  $n$  nodes of a mesh partition of  $\Omega$  into  $p$  elements:

$$\hat{\psi} = \sum_l \psi_l(t) N_l(x, z) \quad \text{for } (x, z) \in R \times R \quad (7)$$

Substituting  $\hat{\psi}$  in the Richards' equation, we generate a residual  $L(\hat{\psi})$  which is minimized by imposing the orthogonality to the functions  $N_l$

$$\int_{\Omega} L(\hat{\psi}) N_l d\Omega = 0, \quad l = 1, n \quad (8)$$

We assume for simplicity that the coordinate directions are parallel to the principal hydraulic anisotropy directions, so that the off-diagonal components of the conductivity tensor are zero. The final system of the spatially-discretized equations is:

$$H(\hat{\psi}) + P(\hat{\psi}) \frac{\partial(\hat{\psi})}{\partial t} + q^*(\hat{\psi}) = 0 \quad (9)$$

where  $H(\hat{\psi})$ ,  $P(\hat{\psi})$ , and  $q^*(\hat{\psi})$  respectively accounts for the hydraulic conductivity, the capillary capacity, and the gravity terms, the latter including also the boundary conditions. Equation (9) is advanced in time by making use of a weighted finite difference scheme, which yields as the final expression:

$$\left( \nu H^{k+\nu} + \frac{P^{k+\nu}}{\Delta t_k} \right) \hat{\psi}^{k+1} = \left( \frac{P^{k+\nu}}{\Delta t_k} - (1-\nu)H^{k+\nu} \right) \hat{\psi}^k + q^{*k+\nu}(\hat{\psi}) \quad (10)$$

where  $H^{k+\nu} = H(\hat{\psi}^{k+\nu})$ ,  $P^{k+\nu} = P(\hat{\psi}^{k+\nu})$ ,  $q^{*k+\nu} = q^*(\hat{\psi}^{k+\nu})$ . The approximate solution at the intermediate time level  $t^{k+\nu}$  is given by  $\hat{\psi}^{k+\nu} = \nu \hat{\psi}^{k+1} + (1-\nu)\hat{\psi}^k$ . The weighting factor  $\nu$  is usually chosen such that  $1/2 \leq \nu \leq 1$ ; the standard choices are  $\nu = 1/2$  for second-order Crank Nicolson scheme and  $\nu = 1$  for first-order backward Euler scheme. The nonlinearities in equation (10), due to the dependence of the terms  $H$ ,  $P$ , and  $q^*$  upon the current approximate solution  $\hat{\psi}^{k+1}$ , demands for some special numerical treatment, such as Picard or Newton iterative methods (Paniconi & Putti, 1994).

Equations (1) and (2) are coupled through the water balance at the interface: the water allowed to infiltrate by the subsurface flow equation gives a contribution as a sink term in the overland flow equation. Evaporation effects are not considered in the present work, since preliminary evaluations ascertained the possibility of neglecting them. The coupling between overland and subsurface flow equations generally introduces a stiffness, which is strictly related to the physical interaction between the two systems. Some special cares in choosing the numerical approximation methods must be carefully deserved in such a critical situation, by adopting suitable iterative solution schemes. However, stiffness is less crucial when the soil is not excessively dry, as in the range we considered in our numerical investigations, and the following simplified algorithm can be applied successfully.

At the  $k$ th-step in time:

- (a) advance from  $t^k$  to  $t^{k+1}$  equation (1) and evaluate the first approximation of  $\bar{h}^{k+1}$  as a function of  $y$ ;
- (b) advance from  $t^k$  to  $t^{k+1}$  equation (2) using the previous estimate of  $\bar{h}(y)$  as a boundary condition and evaluate  $\hat{\psi}^{k+1} = \hat{\psi}(x, z)$ ;
- (c) estimate the infiltration fluxes from the surface to the subsurface system;
- (d) advance again from  $t^k$  to  $t^{k+1}$  equation (1) taking into account the water sink term calculated in (c) and evaluate the final  $\bar{h}^{k+1}$ .

Overland transport phenomena are described by a hyperbolic equation which is formally very similar to that for overland flow. The former equation can thus be spatially and temporally discretized by the same methods adopted for the latter one, i.e. by a shock capturing high-order Godunov-type scheme.

## EXPERIMENTAL PROCEDURE

The preliminary experiments which are presented in this work were performed on a sandy soil with a natural slope of about 9%. The soil consists of about 20% coarse

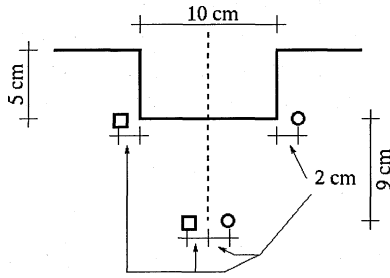


Fig. 2 Vertical section of the rill.

sand, 40% fine sand, 20% very fine sand, 5% coarse silt, 10% fine silt, 5% of clay. The constitutive hydraulic soil relations—retention and unsaturated conductivity—were determined by two 4 m<sup>2</sup> drainage tests at less than 50 m distance. The soil surface was worked to a seedbed-like condition.

The rill was 2 m long. The inflow rates were measured by a flowmeter, were constant in each test and their values are between 15 and 60 \* 10<sup>-3</sup> m<sup>3</sup> h<sup>-1</sup>. An aluminium channel with triangular section and 4.5% slope was used upstream from the rill for regularizing the stream. Energy dissipation meshes were provided at the inlet of the rills.

Six tensiometers were placed at two distances from the axis of the rill and in three transversal sections (Fig. 2). Two 8-mm-diameter stainless steel rods were inserted parallel to the rill axis at 9 cm depth. They were connected to a TDR which was logging every minute the volumetric soil moisture data.

The total mass discharge rate was measured by a load cell at the lower end of the rill. The sediment weight was measured after the trials.

The velocity measurements were made by using a NaCl salt-tracing technique: three pulses were emitted in each experiment, respectively at the beginning, at the

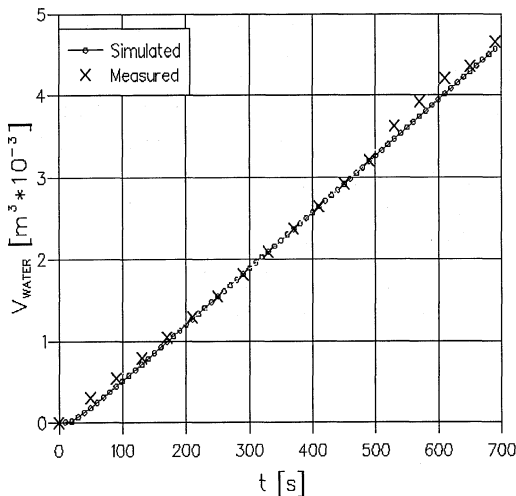
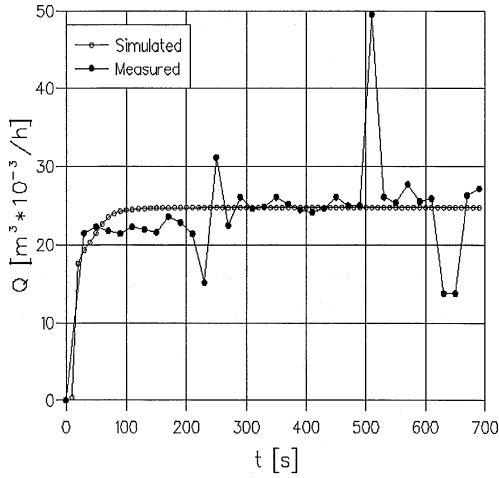
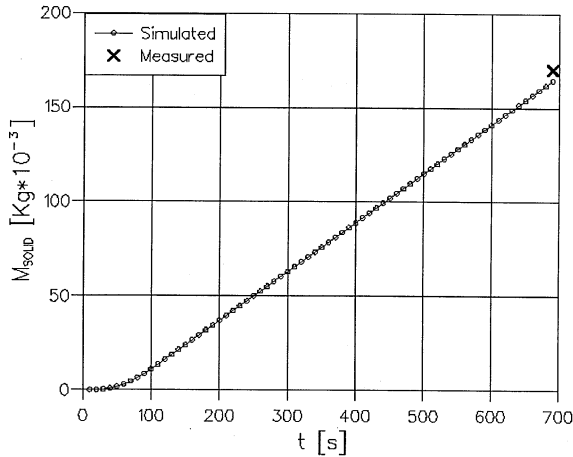


Fig. 3 Volume of water vs time (incoming discharge = 45 m\*10<sup>-3</sup> h<sup>-1</sup>).



**Fig. 4** Discharge of water vs time (incoming discharge =  $45 \text{ m}^3 \cdot 10^{-3} \text{ h}^{-1}$ ).



**Fig. 5** Volume of sediment vs time (incoming discharge =  $45 \text{ m}^3 \cdot 10^{-3} \text{ h}^{-1}$ ).

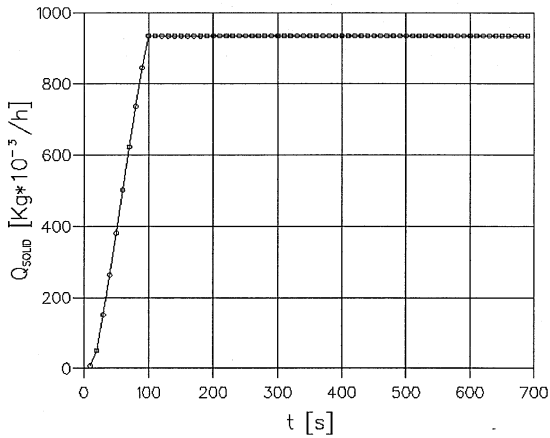


**Fig. 6** Discharge of sediment vs time (incoming discharge =  $45 \text{ m}^3 \cdot 10^{-3} \text{ h}^{-1}$ ).

mean time and at the end at the upper longitudinal side of the rill; the peak in electrical conductivity was detected at the lower longitudinal side of the rill with the two electrodes of a multimeter connected to a PC. A ruler was used for measuring the width of the stream.

## RESULTS AND DISCUSSIONS

Figures 1–6 show good agreement between experimental and numerical results when the upstream water discharge was  $45 \cdot 10^{-3} \text{ m}^3 \text{ h}^{-1}$  and the pressure head in the soil was about 10 cm.

These preliminary results show that the present approach allows an effective numerical simulation of rill soil erosion phenomena. Nevertheless some improvements in the numerical model are required in order to treat low discharges and drier initial conditions. Also, the field experiments should provide the sediment discharge vs time curve.

**Acknowledgement** Dr Gallo was financially supported by Sardinian Regional Authorities.

## REFERENCES

- Brooks, R. H. & Corey, A. T. (1964) Hydraulic properties of porous media. *Hydrology Paper 3, Colorado State University, Fort Collins, Colorado*.
- Colella, P. (1990) Multidimensional upwind methods or hyperbolic conservation laws. *J. Comp. Phys.* **54**, 174–201.
- Hairsine, P. B. & Rose, C. W. (1992) Modeling water erosion due to overland flow using physical principles. 1. Sheet flow. *Wat. Resour. Res.* **28**(1), 237–243.
- Nearing, M. A., Norton, L. D., Bulgakov, D. A., Larionov, G. A., West, L. T. & Dontsova, K. M. (1997) Hydraulics and erosion in eroding rills. *Wat. Resour. Res.* **33**(4), 865–876.
- Paniconi, C. & Putti, M. (1994) A comparison of Picard and Newton iterations in the numerical solution of multidimensional variably saturated flow problems. *Wat. Resour. Res.* **30**(4), 3357–3374.
- Pinder, G. F. & Gray, W. G. (1977) *Finite Element Simulation in Surface and Subsurface Hydrology*. Academic, San Diego, California.
- Sharda, V. N. & Singh, S. R. (1994) A finite element model for simulating runoff and soil erosion from mechanically treated agricultural lands. 1. Governing equations and solutions. *Wat. Resour. Res.* **30**(7), 2287–2298.
- Van Genuchten, M. Th. (1980) A closed form equation for predicting the hydraulic conductivity of unsaturated soils. *Soil Sci. Soc. Am. J.* **44**, 892–898.